PROCEEDINGS of the
23rd International Congress on Acoustics
9 to 13 September 2019 in Aachen, Germany

An impedance model for thin microperforated panels *

Xianhui LI(1), Tuo XING, Liying ZHU, Congshuang JIANG, Wenjiang WANG, Bin ZHANG

Beijing Municipal Institute of Labor Protection, Taoranting Road 55, Beijing 100054, PR China

Abstract

The classical model for the sound absorption of microperforated panels (MPPs) is well developed. For a thin MPP, however, interaction between the air flow on the two sides of the panel may invalidate the impedance end correction in the model. In this paper, a correction length model is proposed to predict the transfer impedance of a thin MPP. Numerical analysis shows that the impedance jumps take place within a distance less than one half of the perforation radius. Provided that the panel thickness is larger than the perforation radius, impedance end correction can be well approximated by adding 1.2 times of the radius to the panel thickness. Sound induced vibration also significantly affects the sound absorption. Herein it is modeled by parallelly connecting the average impedance of a flexible panel to the transfer impedance of a rigid MPP. The experimental results for two different MPP configurations validate the model.

Keywords: Microperforated panels, Impedance model, Sound absorption

1 INTRODUCTION

MPPs were proposed by Maa for efficient sound absorption more than thirty years ago (1-3). The classical MPP model combined the oscillating viscous flow model in small diameter tubes (4, 5) and Ingard's resistive end correction for perforations (6). Recently, many revised models have been proposed to improve the prediction accuracy in the sound absorption. For examples, Allam and Åbom associated the coefficients with edge geometry and used 4 for sharp edge holes and 2 for round edge ones (7). Bolton and Kim found that the coefficient could be better represented as a function of frequency (8). Herdtle et. al. developed a 2D axisymmetric numerical model to simulate a viscous, incompressible, oscillating flow in the time domain (9). They derived an end correction model represented by an additional hole length. Temiz et al. investigated the effect of the edge shape geometry on the end correction using non-dimensional parameters (10). They concluded that the end correction coefficients are functions of the shear wave number and the edge geometry. Based on the viscothermal wave theory (11), Li derived an impedance end correction model for sharp-edged circular perforations (12). It is revealed that a static flow resistance term should be introduced to correctly model the energy dissipation due to the acoustic flow distortion outside the perforation.

The above models have been successfully used in predicting the sound absorption of the MPPs with moderate thicknesses. For a thin MPP, however, interaction between the air flow on the two sides of the panel is not negligible, which may invalidate the impedance end corrections in these models. In this paper, a correction length model is proposed to predict the transfer impedance of a thin MPP. It shows that the impedance jumps take place within the distance less than one half of the perforation radius. Provided that the panel thickness is larger than the perforation radius, contribution from the end effect can be well approximated by adding 1.2 times of the radius to the thickness. Sound induced vibration also significantly affects the transfer impedance. Herein the average impedance of a flexible panel is derived, which is parallelly connected to transfer impedance of a rigid MPP to obtain the overall impedance. Numerical and experimental results validate that the proposed model offers good prediction for the sound absorption of the MPPs.

*(1)Email: lixianh@vip.sina.com

2 MODELING

2.1 Classical MPP model

The classical model was derived from the wave propagation in narrow tubes in which the oscillatory viscous boundary layer spans the hole diameter (1-3). For circular holes, the normal acoustic transfer impedance an MPP with constant-diameter holes can be expressed as

$$Z_{\mathrm{MPP}} = Z_{\mathrm{Perf}} + Z_{\mathrm{End}}, \tag{1}$$

where the impedance due to the perforations is

$$Z_{\mathrm{Perf}} = \frac{j\rho\omega L}{\sigma}\left[1 - \frac{2}{k\sqrt{-j}}\frac{J_1(k\sqrt{-j})}{J_0(k\sqrt{-j})}\right]^{-1}, \tag{2}$$

in which ρ is the density of air, ω is the angular frequency, L is the panel thickness, and σ is the porosity of the MPP. In addition, k is the perforation constant defined as

$$k = r\sqrt{\rho\omega/\eta}, \tag{3}$$

where η is the dynamic viscosity, r is the hole radius, and J_0 and J_1 are the Bessel functions of the first kind of the zeroth and first order, respectively.

The impedance end correction term Z_{End} involves both resistive and reactive parts. Maa (1) used the surface resistance (6), defined by

$$R_s = \sqrt{2\eta\rho\omega}/2 \tag{4}$$

to add resistive end effects and included a reactance correction term derived from the radiation impedance of a piston. The total end correction can written as

$$Z_{\mathrm{End}} = \frac{\rho}{\sigma}\left(\sqrt{\frac{\eta\omega}{2\rho}} + 1.7j\omega r\right). \tag{5}$$

2.2 Correction length model

When the thickness of an MPP is thin enough, the air flow on one side of the panel may interact with that on the other side, which will affect the transfer impedance of the MPP according to (11). In order to investigate the interaction between the air flows, a 2D axisymmetric finite element model is built with the thermoviscous acoustics module of COMSOL Multiphysics®. The setup of the finite element model is shown in Figure 1. The radius of the hole is 0.25 mm, the thickness of the panel is 0.3 mm, and the height of the computational domain is 0.94 mm, which corresponds to a porosity of 7%. A plane wave is incident from the left side and a perfect matched layer is used to reduced of influence of the reflecting wave. On the right side, a plane wave radiation boundary condition is used to model the propagation in a semi-infinite medium.

The normalized impedances of the MPP are computed along the axis of the hole at 250 Hz, 500 Hz, 1000 Hz, 2000 Hz, and 4000 Hz, which are represented by the curves with different colors in Figure 2. One can observe the unit normalized impedances (blue circles) on the right side, which result from a plane wave propagating in an unbounded medium. In the middle of the perforation delimited by two vertical red lines, these curves follow exactly the impedances of the viscous wave in the circular hole given by Equation 2. Near the ends of the hole, there are obvious impedance jumps which take place within a distance much less than one half of the hole radius. Extending the curves in the middle section linearly to the right side, all the lines intersect $Z = 1$ at almost the same position. Its distance from the right end of the hole ΔL is approximately $0.6r$. It is deduced from this observation that the impedance jumps at one end can be approximated by adding the length of the hole by $0.6r$. The impedance jumps at the left end, although slightly different from those at the right end, can

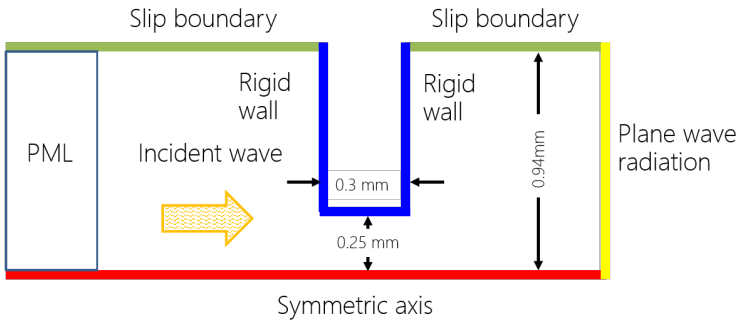

Figure 1. Finite element model setup

be approximately by the same correction length too. Finally, the transfer impedance of the MPP including the end correction can be written as

$$Z_{\mathrm{MPP}} = (1 + 1.2r/L)Z_{\mathrm{Perf}}. \tag{6}$$

The above result is almost identical to the empirical model of Herdtle et. al. (9), where it is obtained from a CFD simulation of an incompressible isothermal flow through a sharp edged straight hole.

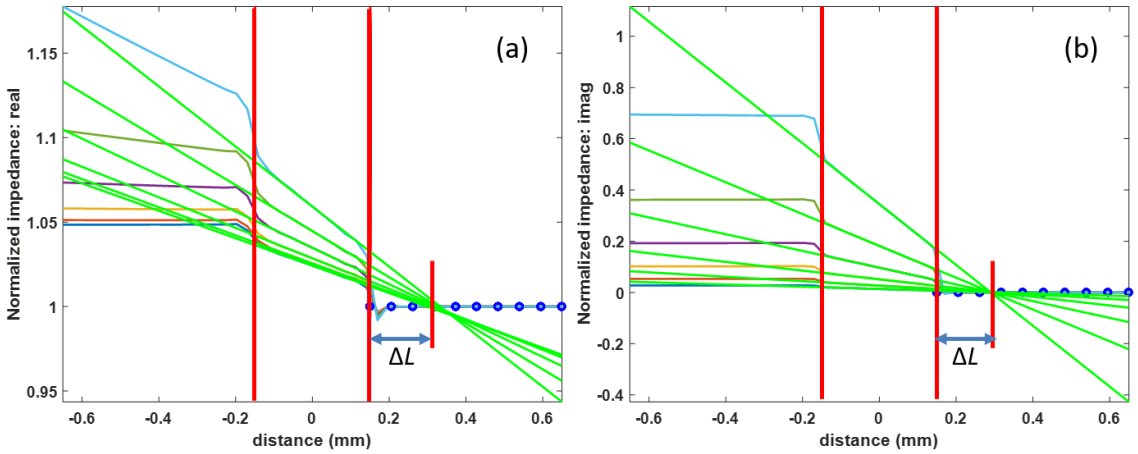

Figure 2. Normalized impedance of an MPP with 0.25 mm radius and 0.3 mm thickness: (a) real part; (b) imaginary part

When the panel thickness is further reduced to 0.15 mm, the normalized impedances are shown in Figure 3. Even though the panel thickness is smaller than the hole radius, the correction length derived above is still valid. Further reducing the panel thickness to 0.1 mm, the impedance jumping regions on the left and right sides begin to merge and different correction lengths are observed for the real and imaginary parts of the impedance, as shown in Figure 4. In such case, the end correction model given by Equation 6 is no longer valid. Fortunately, the thickness of an MPP is seldom less than its perforation radius in practice; hence the air flows on the two sides of the panel can be considered as independent and their influence on the impedance can be approximated by a correction length of $0.6r$ each. This result is in good agreement with that obtained from the time domain simulation of a viscous, incompressible, oscillating flow (9).

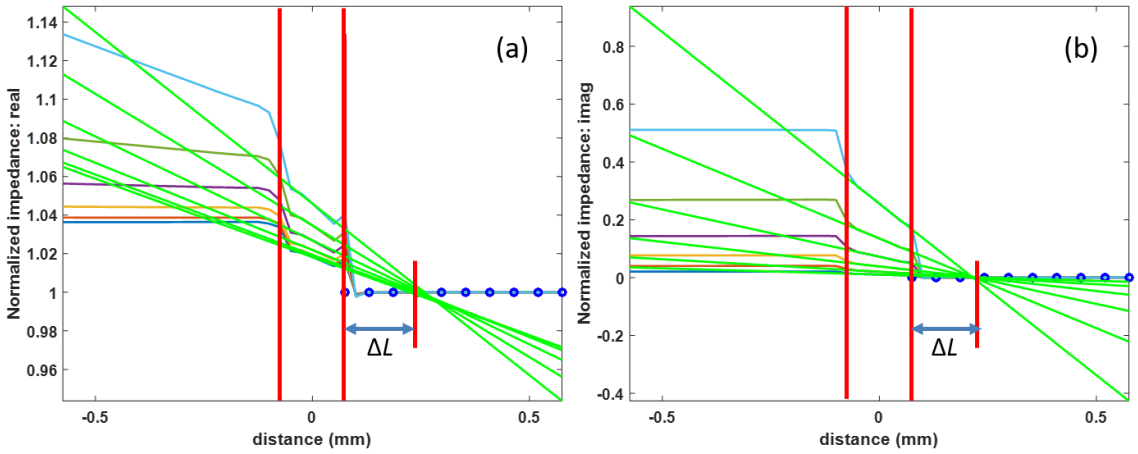

Figure 3. Normalized impedance of an MPP with 0.25 mm radius and 0.15 mm thickness: (a) real part; (b) imaginary part

2.3 Effect of the sound-induced vibration

In this paper, a thin flexible MPP installed in an impedance tube is considered to demonstrate the sound induced vibration effect on the total transfer impedance. Since the size of the MPP is much smaller than the shortest wavelength involved, the incident plane wave approximately exerts a uniform pressure distribution over its surface. Suppose the n^{th} mode shape of the vibrating MPP is $\phi_n(\mathbf{x})$, the average velocity due to the vibration is

$$\bar{v}_{\text{Panel}} = \sum_n \frac{i\omega(\int \phi_n(\mathbf{x})\,dS)^2}{m_n(\omega_n^2 - \omega^2 + 2i\zeta_n\omega\omega_n)} \frac{\Delta p}{S}, \tag{7}$$

where m_n, ω_n, and ζ_n are the modal mass, natural frequency, and modal damping ratio of the n^{th} mode, respectively, Δp is the pressure drop across the MPP, and S is its area.

Due to its small size as compared with the wavelength, the velocity component $\delta v(\mathbf{x}) = v(\mathbf{x}) - \bar{v}_{\text{Panel}}$ of the MPP couples only to the evanescent wave along the normal direction. It follows that the piston-like motion represented by $\bar{v}_{\text{Panel}}$ is sufficient to describe to sound absorption characteristics of the MPP, and an effective impedance is defined as

$$Z_{\text{Panel}} = \frac{\Delta p}{\bar{v}_{\text{Panel}}} = S\left(\sum_n \frac{i\omega(\int \phi_n(\mathbf{x})\,dS)^2}{m_n(\omega_n^2 - \omega^2 + 2i\zeta_n\omega_n\omega)}\right)^{-1}. \tag{8}$$

Taking into account the contribution from the air flow through the perforations, the total average velocity is given according to (13) as

$$\bar{v} = \gamma\bar{v}_{\text{Panel}} + \Delta p/Z_{\text{MPP}}, \tag{9}$$

where $\gamma = 1 - \sigma\text{Im}(Z_{\text{MPP}})/Z_{\text{MPP}}$.

Thus, combining Equations (8) and (9) yields the overall impedance

$$Z_{\text{all}} \equiv \Delta p/\bar{v} = (\gamma/Z_{\text{Panel}} + 1/Z_{\text{MPP}})^{-1}. \tag{10}$$

When the porosity of the MPP is very small, $\gamma \approx 1$ and Z_{all} is actually the parallel connection of Z_{Panel} and Z_{MPP}. Then the normal incident sound absorption coefficient of the absorber is

$$\alpha = \frac{4\rho c\,\text{Re}\{Z_{\text{all}}\}}{(\text{Re}\{Z_{\text{all}}\} + \rho c)^2 + (\text{Im}\{Z_{\text{all}}\})^2}, \tag{11}$$

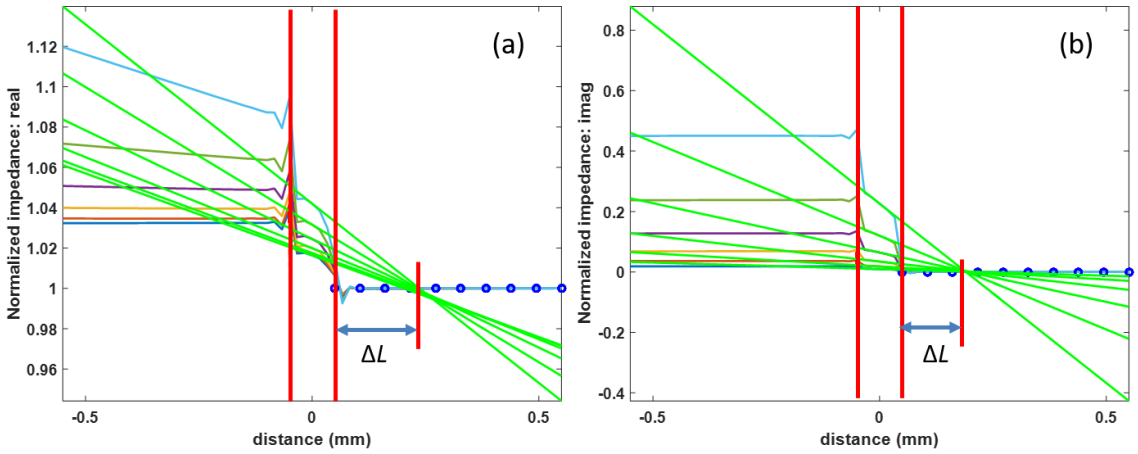

Figure 4. Normalized impedance of an MPP with 0.25 mm radius and 0.1 mm thickness: (a) real part; (b) imaginary part

where c is the air sound speed.

3 VALIDATION

To validate the proposed model, an absorber is made up of a microperforated steel disk of radius 49.8 mm and thickness 0.4 mm, backed by a rigid cylindrical cavity of depth 50 mm. The disk is uniformly perforated by circular holes separated from each other by a distance of 5 mm and with a diameter 0.49 mm. The material has a density of 7800 kg/m^3, Young's modulus 210 GPa, Poisson's ratio 0.3, and modal damping ratio 0.008. The air has a density of 1.21 kg/m^3, sound speed 340 m/s, and dynamic viscosity 1.8×10^{-5} Pa·s. The absorber is installed in a impedance tube and tested according to ISO 10534-2 (14). The frequency range of the measurements is from 200 to 1600 Hz. Figure 5 shows the absorption coefficients of the absorber. It is observed that for the relatively thick MPP the flexural vibration has little effect on the absorber, except a narrow absorption peak at its first axial symmetric mode. In such case, both Maa's model and the proposed model provide good estimations for the sound absorption coefficients.

To highlight the influence of the sound induced vibration on the absorber's performance, another absorber is made up of a microperforated aluminum disk of radius 49.8 mm and thickness 0.2 mm. The disk is uniformly perforated by circular holes separated from each other by a distance of 5 mm and with a diameter 0.48 mm. The material has a density of 2800 kg/m^3, Young's modulus 69 GPa, Poisson's ratio 0.3, and modal damping ratio 0.02. All other parameters remain the same as the first example. Figure 6 shows the absorption coefficients of the absorber. It is observed that the absorption peak is slightly lowered and shifted to a higher frequency due to the sound induced vibration. The proposed model provides better estimations than Maa's model around the sound absorption peaks.

4 CONCLUSIONS

This paper proposed a correction length model to predict the transfer impedance of a thin MPP. It is found from the numerical simulation that the impedance jumps take place within a distance less than one half of the perforation radius. As long as the panel thickness is larger than the perforation radius, contribution from the two ends can be considered independently. Their effects can be well approximated by adding 1.2 times of the perforation radius to the panel thickness. Sound induced vibration also significantly affects the sound

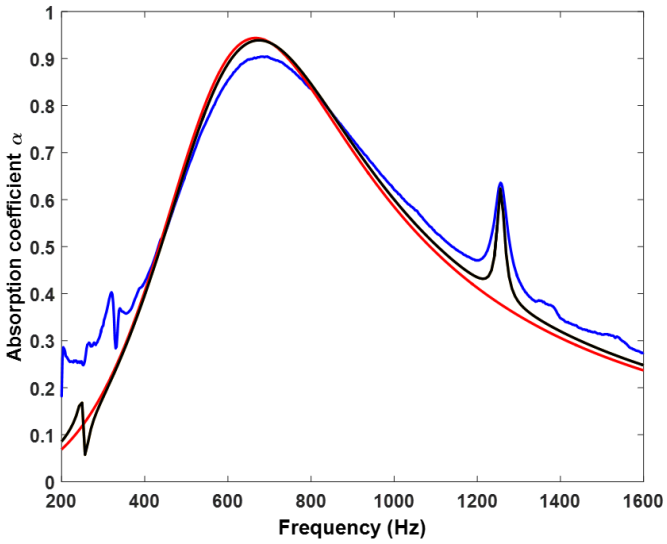

Figure 5. Normal incident sound absorption coefficient of the steel MPP; Experimental data (blue), the proposed model (black), Maa's model (red)

absorption. It can be modeled by parallelly connecting the average impedance of a flexible panel to the transfer impedance of a rigid MPP. Impedance tube test shows that the proposed model offers a good estimation of the sound absorption coefficients of a thin flexible MPP.

ACKNOWLEDGEMENTS

This work is supported by Beijing Natural Science Foundation (1172007), Natural Science Foundation of China (11174041), Xicheng District Excellent Talent Project (20180029, 20180022), Beike Scholar Project (BS201901) and Innovation Project (PXM2019-178304-000003) of BJAST.

REFERENCES

[1] Maa, D. Y. Theory and design of microperforated panel sound-absorbing constructions, Sci. Sin. Vol 18 (1), 1975, pp 55-71.

[2] Maa, D. Y. Microperforated-panel wideband absorbers, Noise Control Eng. J. Vol 29 (3), 1987, pp 77-84.

[3] Maa, D. Y. Potential of microperforated panel absorber, J. Acoust. Soc. Am. Vol 104 (5), 1998, pp 2861-2866.

[4] Rayleigh, J. W. S. The Theory of Sound, Dover Publications, NY (USA), 2nd edition, 1945.

[5] Crandall, I. B. Theory of Vibrating Systems and Sound. Van Nostrand, NY (USA), 1926.

[6] Ingard, U. On the theory and design of acoustic resonators, J. Acoust. Soc. Am. Vol 25 (6), 1953, pp 1037-1061.

[7] Allam, S.; Åbom, M. A new type of muffler based on microperforated tubes, Trans. ASEM, J. Vib. Acoust. Vol 133 (3), 2011, pp 1-8.

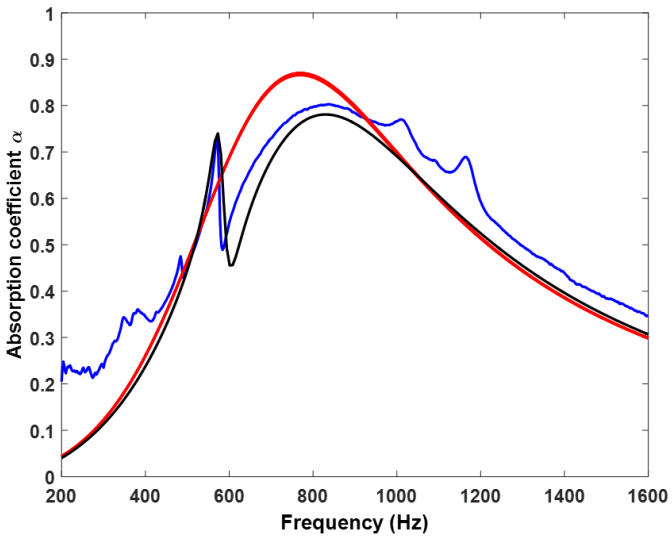

Figure 6. Normal incident sound absorption coefficient of the aluminum MPP; Experimental data (blue), the proposed model (black), Maa's model (red)

[8] Bolton, J. S.; Kim, N. N. Use of CFD to calculate the dynamic resistive end correction for micro-perforated materials, Acoust. Aust. Vol 38, 2010, pp 134-139.

[9] Herdtle, T.; Bolton, J. S.; Kim, N. N.; Alexander, J. H.; Gerdes, R. W. Transfer impedance of microperforated materials with tapered holes, J. Acoust. Soc. Am. Vol 134 (6), 2013, pp 4752-4762.

[10] Temiz, M. A.; Lopez-Arteaga, I.; Efraimsson, G.; Åbom, M.; Hirschberg, A. The influence of edge geometry on end-correction coefficients in micro perforated plates, J. Acoust. Soc. Am. Vol 138 (6), 2015, pp 3668-3678.

[11] Beltman, W. M. Viscothermal wave propagation including acousto-elastic interaction, Part I: Theory, J. Sound Vib. Vol 227 (3), 1999, pp 555-586.

[12] Li, X. End correction model for the transfer impedance of microperforated panels using viscothermal wave theory, J. Acoust. Soc. Am., Vol 141 (3), 2017, pp 1426-1436.

[13] Takahashi, D.; Tanaka, M. Flexural vibration of perforated plates and porous elastic materials under acoustic loading, J. Acoust. Soc. Am., Vol 112 (4), 2002, pp 1456-1464.

[14] International Organization for Standardization, ISO-10534-2: Determination of Sound Absorption Coefficient and Impedance in Impedance Tubes, Geneva, 1998.